J Radioanal Nucl Chem (2014) 299:1759–1766
DOI 10.1007/s10967-014-2920-9

Preparation, molecular modeling and biodistribution of ^{99m}Tc-phytochlorin complex

Mohamed A. Motaleb · Mostafa Y. Nassar

Received: 29 September 2013 / Published online: 22 January 2014

Abstract Phytochlorin [21H, 23H-Porphine-7-propanoicacid, 3-carboxy-5-(carboxymethyl)13-ethenyl-18-ethyl-7, 8-dihydro-2,8,12,17-tetramethyl-,(7S,8S)] was labeled with ^{99m}Tc and the factors affecting the labeling yield of ^{99m}Tc-phytochlorin complex were studied in details. At pH 10, ^{99m}Tc-phytochlorin complex was obtained with a high radiochemical yield of 98.4 ± 0.6 % by adding ^{99m}Tc to 100 mg phytochlorin in the presence of 75 μg $SnCl_2 \cdot 2H_2O$ after 30 min reaction time. The molecular modeling study showed that the structure of ^{99m}Tc-phytochlorin complex presents nearly linear HO–Tc–OH unit with an angle of 179.27° and a coplanar Tc(N1N2N3N4) unit. Biodistribution of ^{99m}Tc-phytochlorin complex in tumor bearing mice showed high T/NT ratio (T/NT = 3.65 at 90 min post injection). This preclinical study showed that ^{99m}Tc-phytochlorin complex is a potential selective radiotracer for solid tumor imaging and afford it as a new radiopharmaceutical suitable to proceed through the clinical trials for tumor imaging.

Keywords Phytochlorin · ^{99m}Tc · SPECT · Tumor · Imaging

Introduction

There is great potential interest in developing new ligands capable of sufficiently selective accumulation in tumors to permit external scintiscanning for tumor diagnosis or delivery of therapeutic radionuclides for tumor-targeted therapy. As one class of derivatives that have special biological functions in the human body's metabolism, porphyrin has received considerable attention due to its specifically distinguish cancer cells from the normal one [1–5].

Porphyrins are essential for many vital and biological functions of normal metabolism of living organisms, such as oxygen transport and storage, photosynthesis, etc. Due to their formation of highly stable and kinetically inert complexes with many metals, they find numerous medical applications [6].

Porphyrin accumulates and causes cellular damage on light excitation, so that it has been used in both detection and treatment of certain malignant tumors by combining porphyrin drugs with light activation [7–9]. The photodynamic therapy (PDT) technique for cancer uses the interaction of a sensitizer and light to destroy cancerous cells and tumors [10].

Several researchers have utilized various porphyrin derivatives and metalloporphyrins for identifying and delineating malignant tissues [11–14]. A wide variety of porphyrin derivatives with various types of peripheral moieties were radiolabeled with several medically important radionuclides to develope a useful porphyrin-based tumor specific agent [6, 15–21].

^{99m}Tc complexes are routinely used in the diagnosis of many cancer diseases involving various organs due to ^{99m}Tc radionuclide has favorable nuclear properties (140 keV, gamma emitters; $t_{1/2}$ = 6:01 h), low cost and readily availability [22, 23].

Phytochlorin[21H,23H-Porphine-7-propanoicacid,3-carboxy-5-(carboxymethyl)13-ethenyl-18-ethyl-7,8-dihydro-2,8,12,17-tetramethyl-,(7S,8S), Fig. 1] is a water soluble porphyrin derivative.

M. A. Motaleb (✉)
Labeled Compounds Department, Hot Lab. Center, Atomic Energy Authority, P.O. Box 13795, Cairo, Egypt
e-mail: mamotaleb10@yahoo.com

M. Y. Nassar
Chemistry Department, Faculty of Science, Benha University, Benha 13518, Egypt

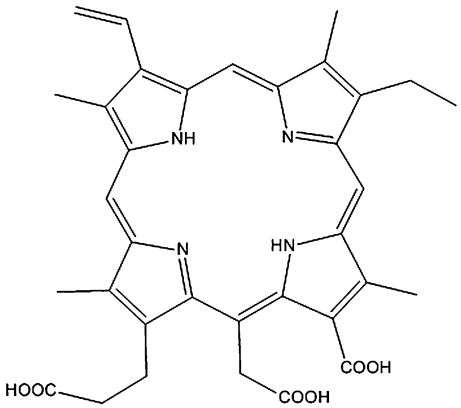

Fig. 1. 21H,23H-Porphine-7-propanoicacid,3-carboxy-5-(carboxymethyl)-13-ethenyl-18-ethyl-7,8-dihydro-2,8,12,17-tetramethyl-,(7S,8S)

The aim of this study is to use ^{99m}Tc for labeling phytochlorin, to evaluate its radiochemical and biological characteristics, and finally to predict the molecular structure of the ^{99m}Tc-phytochlorin complex.

Experimental

Chemicals

Phytochlorin was purchased from Aldrich-Sigma Chemical Company. All other chemicals were purchased from Merck and they were of the highest purity grade.

Radioactive material

^{99m}Tc was eluted as $^{99m}TcO_4^-$ from ^{99}Mo to ^{99m}Tc generator, Elutec Brussels, Belgium.

Methods

Method of labeling

Accurately weighted 100 mg phytochlorin was transferred to an evacuated penicillin vial. N_2-purged stannous chloride aqueous solution (containing exactly 75 μg $SnCl_2{\cdot}2H_2O$) was added and the pH of the mixture was adjusted to 10 then the volume of the mixture was adjusted to 1 mL by N_2-purged distilled water. One mL of freshly eluted $^{99m}TcO_4^-$ (400 MBq) was added to the above reaction mixture. The reaction mixture was then vigorously shaken and allowed to react at room temperature (25 °C) for sufficient time (30 min) to complete the reaction.

Analysis of ^{99m}Tc-phytochlorin complex

The radiochemical purity of ^{99m}Tc-phytochlorin was performed by thin layer chromatographic method using strips of silica gel impregnated glass fiber sheets (ITLC-SG). Free $^{99m}TcO_4^-$ in the preparation was determined using acetone as the mobile phase. Reduced hydrolyzed technetium was determined by using ethanol: water: ammonium hydroxide mixture (2:5:1) as the mobile phase. It was further confirmed by a Shimadzu HPLC system, which consists of pumps LC-9A, UV spectrophotometric detector operated at a 220 nm (SPD-6A), and rheodyne injection valve. Chromatographic analysis of ^{99m}Tc-phytochlorin was performed by injection of 10 μL of the reaction mixture at the optimum conditions into a reversed-phase column, (Waters, Symmetry C18; 5 μm, 4.6 × 150 mm^2) preceded by a guard column (Waters, Symmetry C18; 5 μm) and eluted with mobile phase consisting of acetonitrile and 0.01 M potassium dihydrogen phosphate/diethylamine (60:40:0.2 v/v) [41]. The mobile phase was filtered and degassed prior to use and the flow rate was 0.5 mL/min.

Computational method

The optimized molecular structures of the compound of interest and corresponding energies were calculated by using GAUSSIAN 09 program package [24] using density functional theory with Becke3–Lee–Yang–Parr (B3LYP) [25–27] combined with three different basis sets without any constraint on the geometries. The standard 3-21G basis set was used for carbon and hydrogen atoms and the standard 6-31G basis set was used for oxygen and nitrogen atoms. However, the last basis set was LANL2MB and it was used for technetium atom. The LANL2MB basis set treated electrons near the nuclei via effective core potentials (ECPs) and it also includes some relativistic effect, which are essential for heavy elements like technetium [28–30]. Gaussview program [31] has been considered to get visual the optimized structures. It is worthy to mention that, for the compound of interest, all the optimized structures were found to be true minima, i.e. no imaginary frequency modes were obtained.

Induction of tumor in mice

The parent tumor line (Ehrlich Ascites Carcinoma) was withdrawn from 7 days old donor female Swiss Albino mice and diluted with sterile physiological saline solution to give 12.5 × 10^6 cells/mL. Exactly 0.2 mL solution was injected intramuscularly in the right thigh to produce a solid tumor. The animals were maintained till the tumor development was apparent (10–15 day).

Biodistribution study in mice

In vivo biodistribution studies were carried out in groups of five female Albino mice where each animal was injected in

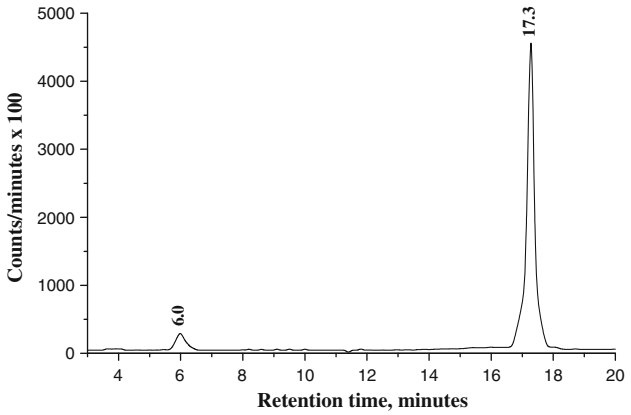

Fig. 2 HPLC radiochromatogram of ^{99m}Tc-phytochlorin complex

the tail vein with 0.2 mL solution containing 5–10 kBq of ^{99m}Tc-phytochlorin. The mice were put in metabolic cages for the required time. The mice were sacrificed by cervical dislocation in groups at various time intervals after injection and the organs or tissues of interest were removed, weighted and counted. To correct for physical decay and to calculate uptake of the radiolabel compound in each tissue sample as a fraction of the injected dose, aliquots of the injected dose were counted simultaneously. The results were expressed as percentage injected dose per gram of tissue or organ (% ID/g).

Results and discussion

The radiochemical yield of ^{99m}Tc-phytochlorin was determined by using thin layer chromatography (TLC-SG) as well as HPLC. Acetone was used with TLC-SG strip to calculate the percentage of free $^{99m}TcO_4^-$ which moved with the solvent front ($R_f = 1.0$) leaving ^{99m}Tc-phytochlorin and colloid at the origin. Ethanol:water:ammonium hydroxide mixture (2:5:1) was used to check the amount of reduced hydrolyzed technetium (colloid) which remained at the origin ($R_f = 0$) while $^{99m}TcO_4^-$ and ^{99m}Tc-phytochlorin migrated with the solvent front ($R_f = 1$). The radiochemical purity was determined by subtracting the sum of the % of colloid and free pertechnetate from 100 %. The radiochemical yield is the mean value of three experiments.

In case of HPLC, an HPLC radiochromatogram is presented in Fig. 2. It exhibited two peaks, one at fraction number 6 corresponding to $^{99m}TcO_4^-$, while the second peak was collected at fraction number 17.3 corresponding to ^{99m}Tc-phytochlorin, which was found to coincide with the UV signal. Nearly, 97 % of the injected activity in the HPLC was recovered as collected activity.

Molecular geometry

It is impossible to determine the exact structure and composition of the reaction product because the amount of ^{99m}Tc eluted from ^{99}Mo/^{99m}Tc generator is very tiny ca. 10^{-9} mol/L [32]. Consequently, we decided to use theoretical background and methods of molecular modeling to predict and design the reaction product. Plus, in order to carry out labeling of the chelating agent with ^{99m}Tc, tin chloride was added to reduce the oxidation state of technetium from IIV to V, IV or III. However, technetium oxidation states in the chelate systems were investigated in presence of $SnCl_2$ and it was concluded and proved that Tc(V) and Tc(IV) were the most stable oxidation states [33, 34]. Moreover, pH of the reaction mixture plays an essential role in the labeling process and in our case it is found that pH 10 is the optimum pH for the labeling process. It is known also that stability of complexes containing chelate rings is more than that of complexes containing none or fewer chelate rings due to the chelate effect [35]. According to this discussion, one can consequently expect the following: Technetium will prefer to coordinate to the four nitrogen atoms of the core of the porphyrine molecule (H_2L) due to the chelate effect; the coordinated technetium atom will complete its coordination sphere with OH^- or O^{2-} species since the optimum pH for the labeling reaction is an alkaline pH; and finally the oxidation state of the coordinated technetium will be +4 or +5. Accordingly, the geometry of the possible complexes {$[LTcO]^+$, **1**; [LTcO], **2**; $[LTcOH]^{2+}$, **3**; $[LTcOH]^+$, **4**; $[(L)OTcO]^-$, **5**; $[(L)OTcO]^{2-}$, **6**; [(L)OTcOH], **7**; $[(L)OTcOH]^-$, **8**; $[(L)HOTcOH]^+$, **9**; and [(L)HOTcOH], **10**} was optimized, in a singlet and doublet state for Tc(V) and Tc(IV) complexes, respectively, by the DFT method with the B3LYP function. The fully optimized geometries of the suggested complexes are shown in Fig. 3. The energy, and dipole moment (μ), for the geometrically optimized complexes are presented in Table 1. It is clear that complex **10** has the lowest energy (−2210.75113006 a.u.) and hence this is the most stable structure for the product of the labeling process. The optimized geometrical structure and the atomic numbering of [(L)HOTcOH], **10**, complex is shown in Fig. 4. The structure of complex **10** presents nearly linear HO–Tc–OH unit with an angle of 179.27° and a coplanar Tc(N1N2N3N4) unit. Some selected parameters of the geometrically optimized structure of complex **10** are presented in Table 2. The calculated bond lengths and angles for Tc–O and Tc–N are in quite good agreement with the values reported for other oxotechnetium and oxorhenium complexes of related structure [36–38].

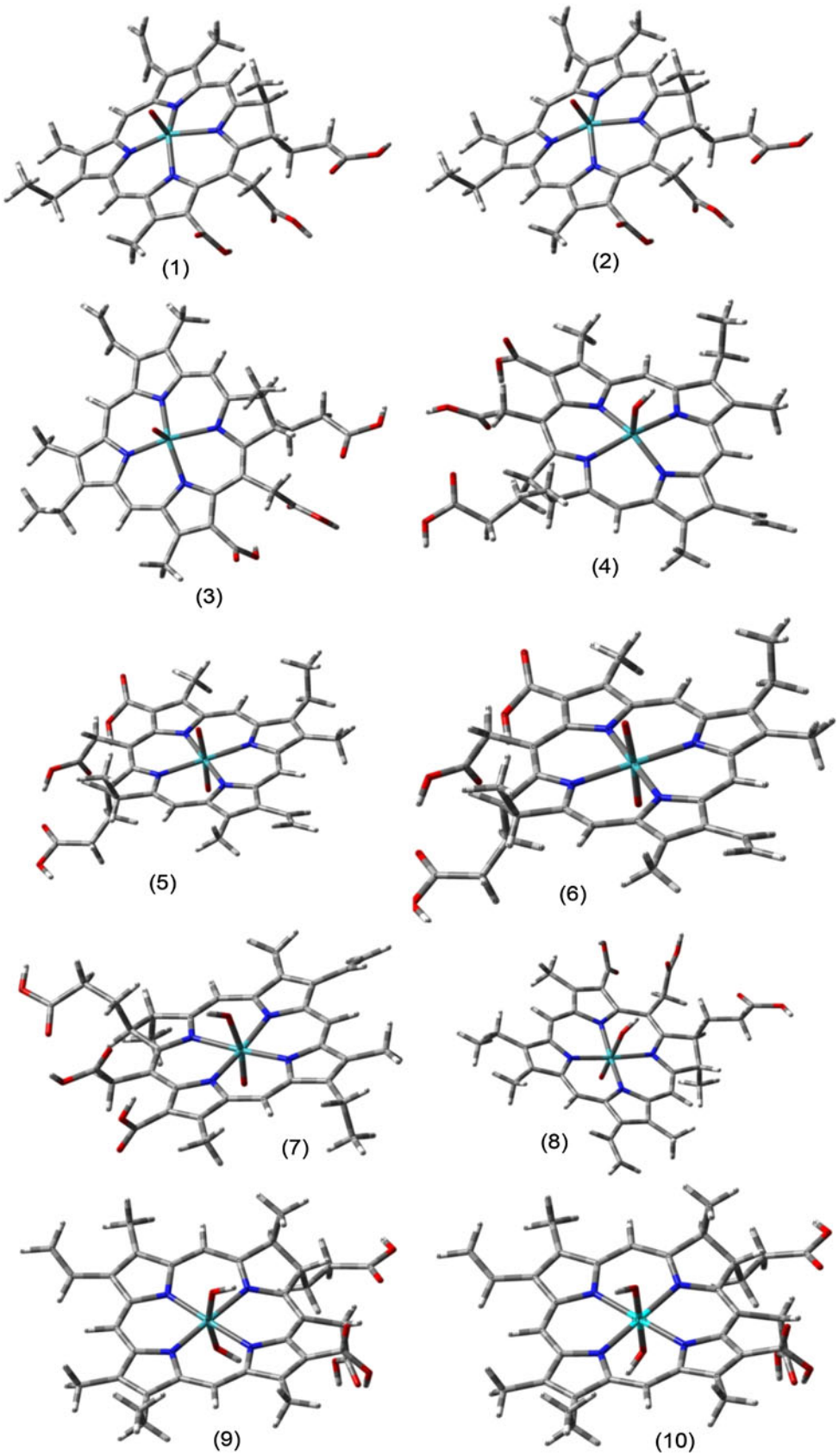

Fig. 3 The geometrically optimized structures of complexes **1–10**

Table 1 Energy and dipole moment for the geometrically optimized structures of possible products

Complex	Energy (a.u.)	μ (Debye)
1	−2,134.58657482	11.875
2	−2,134.77853468	9.746
3	−2,134.92457063	13.768
4	−2,135.13567482	11.354
5	−2,209.59547684	10.035
6	−2,209.78576243	8.243
7	−2,210.13384390	9.485
8	−2,210.20524858	7.245
9	−2,210.52206013	12.589
10	−2,210.75113006	11.354

The labeling conditions for ^{99m}Tc-phytochlorin were studied in detail as follow

Figure 5 shows the effect of phytochlorin amount on labeling yield of ^{99m}Tc-phytochlorin complex. At low phytochlorin concentration (25 mg) the labeling yield was small and equal to 33.2 % where this low labeling yield was due to phytochlorin concentration being insufficient to form the complex with all of the reduced ^{99m}Tc. Increasing the amount of phytochlorin led to higher labeling yield and the maximum yield (98.4 ± 0.6 %) was achieved at 100 mg. By increasing the phytochlorin amount over the optimum value, the labeling yield slightly decreased again till reached 92.5 % at 125 mg phytochlorin.

As shown in Fig. 6, if too much $SnCl_2{\cdot}2H_2O$ content was used, >75 μg, the labeling yield was low (83.5 % at 125 μg $SnCl_2{\cdot}2H_2O$) and the main impurity was reduced hydrolyzed technetium (12.3 % at 125 μg $SnCl_2{\cdot}2H_2O$). This may be due to the fact that most of the ligand molecules are consumed in the formation of complexes, so the pertechnetate is reduced to insoluble technetium (IV) $TcO_2{\cdot}xH_2O$ in the absence of ligand [39] or due to the fact that the excess amount of stannous chloride leads to the formation of stannous hydroxide colloid $Sn(OH)_3^-$ in basic medium [40].

The optimum labeling yield was obtained at 75 μg $SnCl_2{\cdot}2H_2O$ at which a maximum labeling yield was 98.4 ± 0.6 %. Below 75 μg $SnCl_2{\cdot}2H_2O$, stannous chloride is insufficient for complete reduction of pertechnetate to form ^{99m}Tc-phytochlorin complex, this is an explanation of the presence of high quantity of free pertchnetate (59.8 % at 25 μg $SnCl_2{\cdot}2H_2O$).

Figure 7 shows that, the labeling yield of ^{99m}Tc-phytochlorin is dependent on the pH of the reaction mixture in the range from 8 up to 12. The maximum labeling yield of ^{99m}Tc-phytochlorin complex (98.4 ± 0.6 %) was obtained at pH 10. The yield was decreased with decreasing the pH of the reaction mixture with an increase of the $^{99m}TcO_4^-$ (19.3 % at pH 8), above pH 10 the yield decreased again.

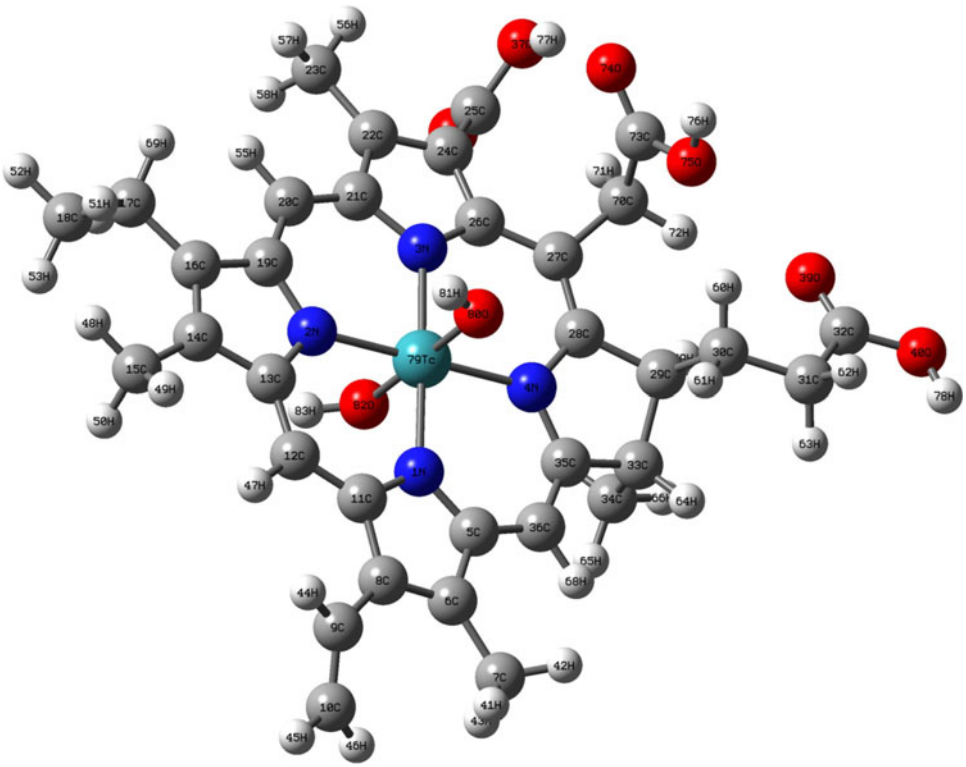

Fig. 4 DFT optimized structure of [(L)HOTcOH], 10, with numbering of atoms

Table 2 Some structure parameters of the optimized geometry of [(L)HOTcOH], 10

Bond length (Å)		Bond angle (°)		Bond dihedral (°)	
N1–Tc79	2.091	N1–Tc79–N2	88.942	C5–N1–Tc79–N2	175.067
N2–Tc79	2.095	N1–Tc79–N4	91.234	C5–N1–Tc79–N4	−4.522
N3–Tc79	2.089	N1–Tc79–O80	90.690	C5–N1–Tc79–O80	−95.064
N4–Tc79	2.104	N1–Tc79–O82	89.434	C5–N1–Tc79–O82	85.655
Tc79–O80	1.929	N2–Tc79–N3	90.689	C11–N1–Tc79–N2	−4.009
Tc79–O82	1.926	N2–Tc79–O80	89.882	C11–N1–Tc79–N4	176.402
O80–H81	0.978	N2–Tc79–O82	89.402	C13–N2–Tc79–N1	3.938
O82–H83	0.978	N3–Tc79–N4	89.125	C13–N2–Tc79–N3	−177.511
		N3–Tc79–O80	90.758	C19–N2–Tc79–N3	3.112
		N3–Tc79–O82	89.107	C35–N4–Tc79–N1	7.692
		N4–Tc79–O80	90.527	C35–N4–Tc79–N3	−170.856
		N4–Tc79–O82	90.189	C35–N4–Tc79–O80	98.394
		O80–Tc79–O82	179.269	C35–N4–Tc79–O82	−81.752
		Tc79–O80–H81	121.877		
		Tc79–O82–H83	123.148		

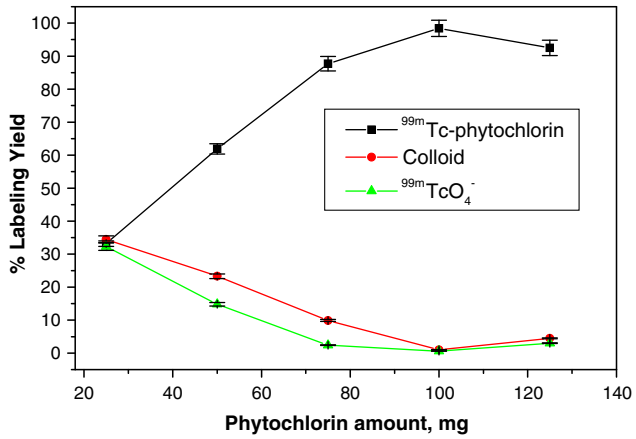

Fig. 5 Effect of phytochlorin amount on percent labeling yield of ^{99m}Tc-phytochlorin

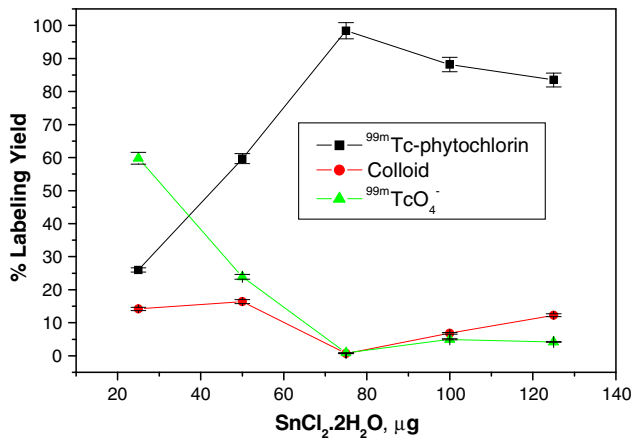

Fig. 6 Effect of $SnCl_2{\cdot}2H_2O$ on percent labeling yield of ^{99m}Tc-phytochlorin

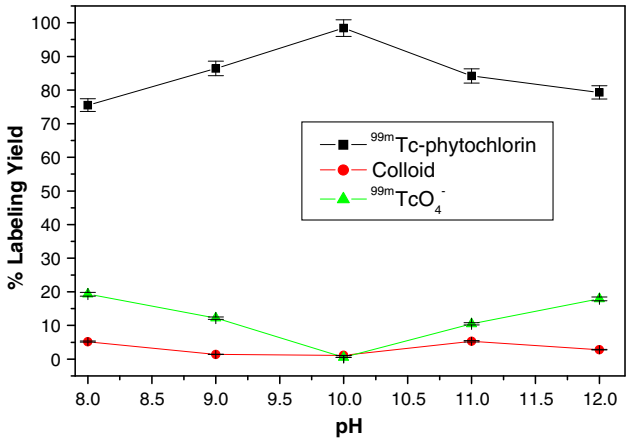

Fig. 7 Effect of pH of the reaction mixture on percent labeling yield of ^{99m}Tc-phytochlorin

The stability of ^{99m}Tc-complex was studied in order to determine the suitable time for injection to avoid the formation of the undesired products that result from the radiolysis of the labeled compound. These undesired radioactive products may be accumulated in non-target organs. Figure 8 shows the effect of reaction time on percent labeling yield of ^{99m}Tc-phytochlorin where at 15 min, the labeling yield of ^{99m}Tc-phytochlorin complex was low and maximized (98.4 ± 0.6 %) at 30 min then the labeling yield remained stable up to 8 h.

Biodistribution of ^{99m}Tc-phytochlorin complex

Biodistribution of ^{99m}Tc-phytochlorin in solid tumor bearing mice is shown in Table (3). Biodistribution assay was done at time intervals 20, 60, 90 and 120 min p.i. and the results were

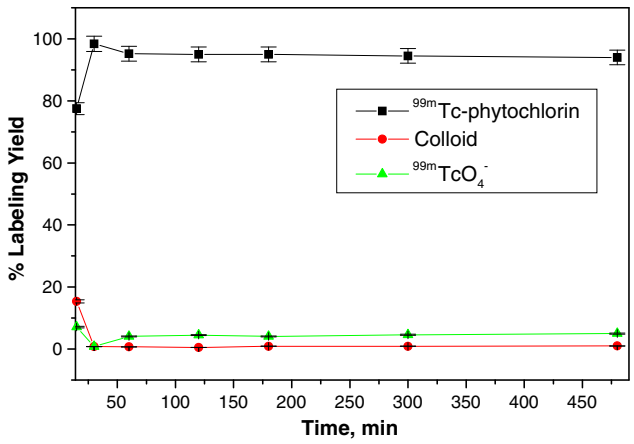

Fig. 8 Radiochemical stability of ^{99m}Tc-phytochlorin complex

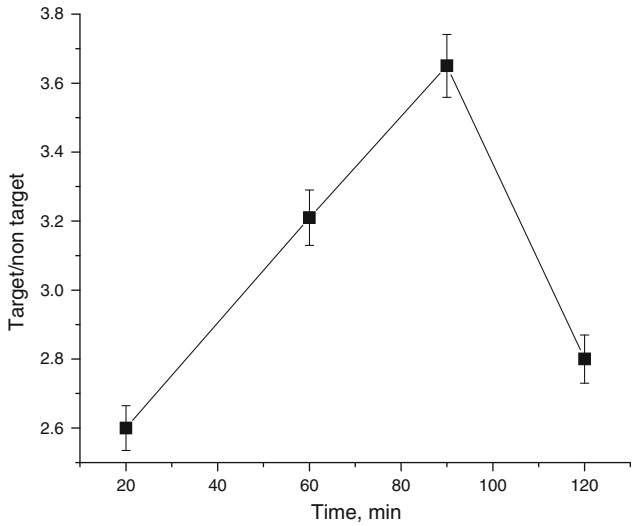

Fig. 9 T/NT ratio of ^{99m}Tc-phytochlorin in solid tumor bearing mice

expressed as % injected dose per gram organ or fluid (%ID/g organ). The body clearance of ^{99m}Tc-phytochlorin is mainly through the urinary pathway and the activity is not accumulated in specific organ other than the solid tumor tissue. The selectivity of ^{99m}Tc-phytochlorin was evaluated by the target/non-target (T/NT) ratio between tumor muscle (right mouse thigh muscle) and normal muscle (left mouse thigh muscle). Figure 9 shows T/NT ratio of ^{99m}Tc-phytochlorin in solid tumor bearing mice which clarify that ^{99m}Tc-phytochlorin is highly selective to the tumor cells with an accumulation ratio 3.65 at 90 min post injection. T/NT ratio of ^{99m}Tc-phytochlorin is higher than that of many other radiopharmaceuticals such as ^{99m}Tc-DETA, ^{99m}Tc-TETA, ^{99m}Tc-TEPA, [^{99m}Tc(CO)$_3$(IDA–PEG3–CB)]$^-$, ^{99m}Tc-nitride-pyrazolo[1,5-a]pyrimidine and ^{99m}Tc-HL-91 and ^{99m}Tc-2-methoxy-isobutyl-isonitrile [41–45]. This preclinical study suggests that ^{99m}Tc-phytochlorin is a selective agent for solid tumor imaging and can be used as a potential solid tumor imaging radiotracer.

Conclusion

^{99m}Tc-phytochlorin can easily be labeled with high labeling yield of 98.4 ± 0.6 % by direct labeling technique using $SnCl_2{\cdot}2H_2O$ as a reducing agent. The molecular modeling study of the labeled compound showed that the structure of ^{99m}Tc-phytochlorin complex has nearly linear HO–Tc–OH unit with an angle of 179.27° and a coplanar

Table 3 In vivo biodistribution study of ^{99m}Tc-phytochlorin in solid tumor bearing Albino mice at different time intervals post injection, (% ID/g organ ± SE, $n = 3$)

Body organ (fluid)	% Injected dose/g organ (fluid) at time intervals, min			
	20	60	90	120
Blood	12.02 ± 0.41	6.51 ± 0.10	3.14 ± 0.03	1.5 ± 0.01
Kidneys	18.2 ± 0.33	23.21 ± 0.17	28.17 ± 2.31	39.9 ± 0.94
Liver	2.64 ± 0.14	3.9 ± 0.12	6.37 ± 0.3	8.14 ± 0.31
Spleen	2.11 ± 0.1	1.83 ± 0.03	1.32 ± 0.05	1.08 ± 0.03
Intestine	3.88 ± 0.06	4.24 ± 0.11	6.5 ± 0.22	8.02 ± 0.04
Stomach	0.8 ± 0.01	1.2 ± 0.22	3.21 ± 0.24	6.2 ± 0.13
Lungs	7.5 ± 0.26	5.37 ± 0.23	3.71 ± 0.11	2.16 ± 0.02
Heart	4.95 ± 0.31	2.22 ± 0.03	1.06 ± 0.02	0.87 ± 0.01
Bone	2.02 ± 0.21	1.98 ± 0.2	1.72 ± 0.04	1.09 ± 0.06
Tumor muscle	7.31 ± 0.25	2.82 ± 0.12	2.99 ± 0.13	2.29 ± 0.11
Normal muscle	2.81 ± 0.08	0.88 ± 0.02	0.82 ± 0.02	0.82 ± 0.02
T/NT	2.6	3.21	3.65	2.8

Tc(N1N2N3N4) unit. Moreover, the biodistribution studies of ^{99m}Tc-phytochlorin revealed that ^{99m}Tc-phytochlorin has high T/NT ratio and is rapidly cleared out from body organs and excreted via the urinary pathway. These findings, combined with the advantage of the high labeling yield and stability of ^{99m}Tc-phytochlorin complex, are promising enough to encourage clinical investigation of this new ^{99m}Tc agent as a selective potential radiopharmaceutical for solid tumor imaging.

References

1. Figge FHJ, Weiland GS, Manganiello LOJ (1948) Proc Soc Exp Biol Med 68:640
2. Altman KF, Solomon K (1960) Nature 187:1124
3. Lipson RL, Baldes EJ, Gray MS (1967) Cancer 20:2255
4. Sanderson DR, Fontana RS, Lipson RL, Baldes EJ (1972) Cancer 30:1368
5. Zhiyun J, Houfu D, Manfei P (2007) Nucl Med Biol 34:643
6. Biesaga M, Pyrzynska K, Trojanowicz M (2000) Talanta 51:209
7. Ko YJ, Yun KJ, Kang MS, Park J, Lee KT, Park SB, Shin JH (2007) Bioorg Med Chem Lett 17:2789
8. Kolarova H, Macecek J, Nevrelova P, Huf M, Tomecka M, Bajgar R, Mosinger J, Strnad M (2005) Toxicol In Vitro 19:971
9. Kessel D (2004) Photodiagn Photodyn Ther 1:3
10. Asta J, Johan M (2007) Photodiagn Photodyn Ther 4:3
11. Fawwaz R, Bohdiewicz P, Lavallee D, Wang T, Oluwole S, Newhouse J, Alderson A (1990) Nucl Med Biol 17:65
12. Subbarayan M, Shetty SJ, Srivastava TS, Noronha OPD, Samuel AM, Mukhtar H (2001) Biochem Biophys Res Commun 281:32
13. Banerjee S, Das T, Samuel G, Sarma HD, Venkatesh M, Pillai MRA (2001) Nucl Med Commun 22:1101
14. Das T, Chakraborty S, Sarma HD, Banerjee S (2008) Radiochim Acta 96:427
15. Hambright P, Fawwaz RA, Valk P, McRae J, Bearden (1975) Bioinorg Chem 5:87
16. Zanelli GD, Kaelin AD (1981) Br J Radiol 54:403
17. Whelan HT, Kras LH, Ozker K, Bajic D, Schmidt MH, Liu Y, Trembath LA, Uzum F, Meyer GA, Segura AD, Collier BD (1994) J Neurooncol 22:7
18. Bhalgat MK, Roberts JC, Mercer-Smith JA, Knotts BD, Vessella RL, Lavallee (1997) Nucl Med Biol 24:179
19. Subbarayan M, Shetty SJ, Srivastava TS, Noronha OPD, Samuel AM (2001) J Porphyr Phthalocyanines 5:824
20. Kavali RR, Lee BC, Moon BS, Yang SD, Chun KS, Choi CW, Lee C-H, Chi DY (2005) J Label Compd Radiopharm 48:749
21. Jia Z, Deng H, Pu M (2007) Nucl Med Biol 34:643
22. Jurisson S, Bering D, Jia W, Ma D (1993) Chem Rev 93:1137
23. Jurisson SS, Lydon JD (1999) Chem Rev 99:2205
24. Frisch MJ, Trucks GW, Schlegel HB, Scuseria GE, Robb MA, Cheeseman JR, Scalmani G, Barone V, Mennucci B, Petersson GA, Nakatsuji H, Caricato M, Li X, Hratchian HP, Izmaylov AF, Bloino J, Zheng G, Sonnenberg JL, Hada M, Ehara M, Toyota K, Fukuda R, Hasegawa J, Ishida M, Nakajima T, Honda Y, Kitao O, Nakai H, Vreven T, Montgomery Jr JA, Peralta JE, Ogliaro F, Bearpark M, Heyd JJ, Brothers E, Kudin KN, Staroverov VN, Keith T, Kobayashi R, Normand J, Raghavachari K, Rendell A, Burant JC, Iyengar SS, Tomasi J, Cossi M, Rega N, Millam JM, Klene M, Knox JE, Cross JB, Bakken V, Adamo C, Jaramillo J, Gomperts R, Stratmann RE, Yazyev O, Austin AJ, Cammi R, Pomelli C, Ochterski JW, Martin RL, Morokuma K, Zakrzewski VG, Voth GA, Salvador P, Dannenberg JJ, Dapprich S, Daniels AD, Farkas O, Foresman JB, Ortiz JV, Cioslowski J, Fox DJ (2010) Gaussian 09, Revision C.01. Gaussian, Wallingford
25. Becke AD (1993) J Chem Phys 98:5648
26. Lee C, Yang W, Parr RG (1988) Phys Rev B 37:785
27. Stephens PJ, Devlin FJ, Chabalowski CF, Frisch MJ (1994) J Phys Chem 98:11623
28. Hehre WJ, Stewart RF, Pople JA (1969) J Chem Phys 51:2657
29. Collins JB, Schleyer PVR, Binkley JS, Pople JA (1976) J Chem Phys 64:5142
30. Hay PJ, Wadt WR (1985) J Chem Phys 82:299
31. Computer program GaussView Version 5.0.9. Gaussian, Wallingford
32. Stanik R, Benkovsky I (2011) J Radioanal Nucl Chem 287:949
33. Fišer M, Brabec V, Dragoun O, Lázníčkova A, Kovalík A, Ryšavy M (1985) Int J Appl Radial Isot 36:1213
34. Fišer M, Brabec V, Dragoun O, Kovalík A, Frana J, Ryšavy M (1985) Int J Appl Radial Isot 36:219
35. Cotton FA, Wilkinson G, Murillo CA, Bochmann M (1999) Advanced inorganic chemistry, 6th edn. Wiley, New York
36. Liu S, Rettig SJ, Orvig C (1991) Inorg Chem 30:4915
37. Chatterjee S, Del Negro AS, Wang Z, Edwards MK, Skomurski FN, Hightower SE, Krause JA, Twamley B, Sullivan BP, Reber C, Heineman WR, Seliskar CJ, Bryan SA (2011) Inorg Chem 50:5815
38. Gancheff J, Kremer C, Kremer E, Ventura ON (2002) J Mol Struct Theochem 580:107
39. Srivastava SC, Richards P (1983) Technetium-labled compounds. In: Rayudu GVS (ed) Radiotracers for medical applications, CRC series in radiotracers in biology and medicine. CRC Press, Boca Raton, p 107
40. Wardell JL (1994) Tin: inorganic chemistry. In: King RB (ed) Encyclopedia of inorganic chemistry, vol 8. Wiley, New York, p 4159
41. Wan W, Yang M, Pan S, Yu C, Wu N (2008) Drug Dev Res 69:520
42. Wang J, Yang J, Yan Z, Duan X, Tan C, Shen Y, Wu W (2011) J Radioanal Nucl Chem 287:465
43. Ding R, He Y, Xu J, Liu H, Wang X, Feng M, Qi C, Zhang J, Peng C (2012) Med Chem Res 21:523
44. Hsia C, Huang F, Lin C, Shen L, Wanga H (2010) Appl Radiat Isot 68:1610
45. Abrantes AM, Serra ME, Gonçalves AC, Rio J, Oliveiros B, Laranjo M, Rocha-Gonsalves AM, Sarmento-Ribeiro AB, Botelho MF (2010) Nucl Med Biol 37:125